

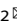


ARTICLE



Homozygous variant in *DRC3* (*LRRC48*) gene causes asthenozoospermia and male infertility

Jiao Qin^{1,2}, Jinyu Wang³, Jianhai Chen⁴, Jinyan Xu^{1,2}, Shanling Liu³, Dong Deng⁵ and Fuping Li^{1,2}

© The Author(s), under exclusive licence to The Japan Society of Human Genetics 2024

Human infertility affects 10–15% of couples. Asthenozoospermia accounts for 18% of men with infertility and is a common male infertility phenotype. The nexin-dynein regulatory complex (N-DRC) is a large protein complex in the sperm flagellum that connects adjacent doublets of microtubules. Defects in the N-DRC can disrupt cilia/flagellum movement, resulting in primary ciliary dyskinesia and male infertility. Using whole-exome sequencing, we identified a pathological homozygous variant of the dynein regulatory complex subunit 3 (*DRC3*) gene, which expresses leucine-rich repeat-containing protein 48, a component of the N-DRC, in a patient with asthenozoospermia. The variant ENST00000313838.12: c.644dup (p. Glu216GlyfsTer36) causes premature translational arrest of *DRC3*, resulting in a dysfunctional *DRC3* protein. The patient's semen count, color, and pH were normal according to the reference values of the World Health Organization guidelines; however, sperm motility and progressive motility were reduced. *DRC3* protein was not detected in the patient's sperm and the ultrastructure of the patient's sperm flagella was destroyed. More importantly, the *DRC3* variant reduced its interaction with other components of the N-DRC, including dynein regulatory complex subunits 1, 2, 4, 5, 7, and 8. Our data not only revealed the essential biological functions of *DRC3* in sperm flagellum movement and structure but also provided a new basis for the clinical genetic diagnosis of male infertility.

Journal of Human Genetics; <https://doi.org/10.1038/s10038-024-01253-6>

INTRODUCTION

As a widespread health issue, human infertility affects 10–15% of couples. Infertility is defined as the inability to achieve a clinical pregnancy for one year despite having a normal sex life without contraception [1]. Male factors are thought to account for half of all infertility cases. Male infertility is mainly diagnosed as azoospermia (no sperm is found in two consecutive semen examinations), asthenozoospermia (sperm progressive motility < 32% or total motility < 40%), oligozoospermia (sperm concentration < 15 × 10⁶/mL), teratozoospermia (normal sperm morphology < 4%), or a combination of these defects [2]. Asthenozoospermia is a common phenotype of male infertility, accounting for 18% of patients with infertility [3].

Normal sperm movement depends on its structure, and defects of sperm tail structure could result in a deficiency in sperm movement. The sperm axoneme is evolutionarily highly conserved and is the structural basis of sperm motility [4]. Regulatory complexes are required to maintain the regular beating of flagella. The nexin-dynein regulatory complex (N-DRC) is among the most important complexes [5]. It is a large protein complex consisting of at least 11 subunits (DRC1–DRC11), which is highly conserved from *Chlamydomonas* to humans [6]. However, a recent study identified the DRC12 subunit in *Tetrahymena thermophila* [7]. The N-DRC connects adjacent doublets of microtubules (DMTs), forming a bridge between the A and B submicrotubules [6, 8].

Dynein regulatory complex subunit 3 (*DRC3*) is a functional subunit of the N-DRC located on the flagellar axoneme of the *Chlamydomonas*. The human *DRC3* gene expresses leucine-rich repeat (LRR)-containing protein 48 (*LRRC48*) [9]. A recent study found two mutations (c.1308_1311del and c.1031delT) in two patients with multiple morphological abnormalities of the flagella (MMAF) phenotype and obstructive azoospermia [10]. However, whether *DRC3* deficiency can cause other phenotypes remains unclear, as does the functional role of *DRC3* in male reproduction. In addition, more mutations need to be identified in men with infertility to provide a basis for the clinical genetic diagnosis of male infertility.

In this study, we performed whole-exome sequencing of 30 unrelated men with infertility with asthenozoospermia (20 presented with the MMAF phenotype, and 10 presented with only asthenozoospermia), and identified a pathological homozygous variant in the *DRC3* (*LRRC48*) gene in a patient with asthenozoospermia. The variant ENST00000313838.12: c.644dup (p.Glu216GlyfsTer36) results in a dysfunctional *DRC3* protein because of the premature translational arrest of *DRC3*. The morphology of the patient's sperm flagella was normal; however, the ultrastructure was destroyed. Furthermore, this variant reduced the interaction between *DRC3* and other N-DRC components. Overall, our findings demonstrated that mutations in *DRC3* are most likely the underlying cause of male infertility in a subgroup of individuals with asthenozoospermia, providing a new basis for the genetic diagnosis of male infertility.

¹Department of Andrology/Sichuan Human Sperm Bank, West China Second University Hospital, Sichuan University, Chengdu, China. ²Key Laboratory of Birth Defects and Related Diseases of Women and Children (Sichuan University), Ministry of Education, Chengdu, China. ³Department of Medical Genetics, West China Second University Hospital of Sichuan University, Chengdu 610041, China. ⁴Department of Ecology and Evolution, Biological Sciences Division, The University of Chicago, 1101 E 57th Street, Chicago, IL 60637, USA. ⁵Department of Obstetrics, Key Laboratory of Birth Defects and Related Disease of Women and Children of MOE, State Key Laboratory of Biotherapy, West China Second Hospital, Sichuan University, Chengdu 610041, China. ✉email: sunny630@126.com; dengd@scu.edu.cn; lfpsnake@scu.edu.cn

Received: 16 November 2023 Revised: 16 April 2024 Accepted: 16 April 2024

Published online: 20 May 2024

MATERIALS AND METHODS

Study participants

A cohort of 30 Chinese men with MMAF (short, absent, coiled, bent, or irregular flagella) or asthenozoospermia (total sperm motility < 40% and no obvious MMAF phenotype) was enrolled from the Department of Andrology/Sichuan Human Sperm Bank, West China Second University Hospital. All enrolled patients exhibited primary infertility; those with primary ciliary dyskinesia were excluded. Karyotypic analyses of all the enrolled patients revealed normal karyotypes (46XY), hormone levels, bilateral testicular size distributions, and secondary sex characteristics. The patients and healthy controls provided informed consent, and the Ethics Committee of the West China Second University Hospital approved the study. Blood and semen samples were collected from the patients.

Semen analysis

In line with the World Health Organization (WHO) guidelines (fifth edition), human sperm samples were collected by masturbation into sterile semen cups after abstinence for two to seven days. Sperm samples were incubated at 37 °C until liquefaction and were evaluated within 1 h. During routine clinical diagnosis, standard parameters, including semen volume, concentration, motility, progressive motility and morphology were assessed. More than 200 spermatozoa from each individual were counted to evaluate the proportion of morphologically abnormal sperm.

Whole-exome sequencing and Sanger sequencing

DNA was extracted from whole peripheral blood of all patients using a DNeasy Blood and Tissue kit (QIAGEN, Dusseldorf, Germany). Exonic sequences were isolated and enriched using SureSelectXT Human All Exon Kit (Agilent Technologies). Samples were sequenced on an Illumina HiSeq X-TEN platform. Read mapping (Burrows–Wheeler Aligner, BWA v0.7.17), calling (Genome Analysis Toolkit, v4.1), genotyping, and annotation (ANNOVAR and VEP) were performed as part of the sequencing analyses, as detailed previously [11–14].

Antibodies

Rabbit LRRC48 (DRC3) antibody fluorescein isothiocyanate (FITC), which detects the N-terminus of DRC3, was obtained from Universal Biotech Co., Ltd. (Shanghai, China). Alpha tubulin monoclonal antibody (AF594), mice HA, MYC, FLAG, Strep-tag monoclonal antibodies, β -tubulin, and actin antibodies were obtained from Proteintech (Wuhan, China) [15, 16].

Plasmids

Human *DRC3*, *DRC4*, and *DRC5* coding sequences were obtained from National Center for Biotechnology Information, and a mutated form of *DRC3* (*DRC3* MU) was designed based on the mutation identified in the patient. We constructed an MYC tag at the N-terminus of the *DRC3* wild type (WT) and mutated form (MU), FLAG tag and HA tag at the N-terminus of *DRC4* and *DRC5* respectively. *DRC1*, 2, 7, and 8 were added to the Strep-tag at the N-terminus. All genes were cloned into the pcDNA3.0 vector with the HindIII–XhoI restriction enzyme site, and all plasmids were synthesized by Zhejiang Youkang Biotechnology Co., Ltd. (Zhejiang, China).

Papanicolaou staining

Papanicolaou staining was used to stain the sperm after the semen was liquefied. We counted more than 200 sperm to calculate the proportion of sperm with normal morphology.

Protein extraction and western blot

MYC tag *DRC3* WT; MYC tag *DRC3* MU; FLAG tag *DRC4*; HA tag *DRC5*; and Strep tag *DRC1*, 2, 7, and 8 were transfected into HEK 293 suspension (293 F) cells, and the cells were collected after 72 h. Cells were lysed using phosphate-buffered saline (PBS) lysis buffer (PBS buffer, pH 7.5, 1% Triton X-100). Immunoprecipitation was performed using protein A/G magnetic beads following the manufacturer's instructions. Each immunoprecipitation solution contained 1 mL of cell lysate and 1 μ L of tag antibody. After overnight incubation at 4 °C, the resin was washed five times with 1 mL cold lysis buffer. In each group, 50 μ L of magnetic beads suspension was used for western blot. The samples were heated at 100 °C for 10 min, subjected to SDS-PAGE, and transferred onto PVDF membranes. Membranes were blocked in 5% fat-free milk in Tris-buffered saline at 25 °C for 2 h and then incubated overnight in the relevant primary antibodies at 4 °C. After washing

with TBST (1 \times Tris-buffered saline, 0.1% Tween® 20 detergent), the membranes were incubated with the corresponding secondary antibodies for 2 h at 25 °C and rinsed with TBST. The protein blots were visualized using a chemiluminescence imaging system (BOX Chemi XPQ).

Scanning and transmission electron microscopy

We used scanning electron microscopy (SEM) and transmission electron microscopy (TEM) to analyze spermatozoa surface and ultrastructural abnormalities in detail. Samples for SEM were washed with PBS, smeared on a coverslip, and then put into a six-well plate. After the samples had dried, they were fixed with 3% glutaraldehyde at 4 °C. For TEM, samples were first rinsed with PBS and fixed with 0.5% glutaraldehyde at 4 °C for 10 min. After centrifugation at 25 °C and 1500 rpm for 15 min, the supernatant was discarded, and 3% glutaraldehyde was added for fixation. All samples were tested and photographed at Chengdu Lilai Biotechnology (Chengdu, China).

Immunofluorescence

Sperm samples were washed with PBS, fixed with 4% paraformaldehyde for 15 min, and permeabilized with 0.5% Triton X-100 for 10 min. Then, following blocking with 5% skim milk powder in Tris-buffered saline buffer for 1 h, the samples were incubated overnight with fluorescence conjugated antibodies at 4 °C and washed with TBST. The sperm nuclei were stained with DAPI (4',6'-diamidino-2-phenylindole) at 37 °C for 5 min. Images were captured using an LSM 800 confocal microscope (Carl Zeiss AG).

Quantitative real-time PCR

A human MTC Panel II was purchased from Clontech (catalog number: 636743; Takara, Beijing, China) and analyzed using a ChamQ SYBR® qPCR Master Mix kit (Vazyme, Nanjing, China). Thermocycler settings were as follows: 50 °C for 2 min, 95 °C for 5 min, and 40 cycles of 95 °C for 10 s and 60°C for 30 s. The *DRC3* primers were as follows: 5' (upstream) primer, 5'-TTCTGACTCCCTAGCAAC-3', and 3' (downstream) primer, 5'-GAGTTCAGGAGTCAAGACCAG-3'. We chose human *G3PDH* as the control, the primers were as follows: 5' (upstream) primer, 5'-TGAAGGTCGGAGTCAACGGATTGGT-3', and 3' (downstream) primer, 5'-CATGTGGCCATGAGGTCCACCAC-3'.

RESULTS

Identification of a homozygous mutation of *DRC3* in a patient with asthenozoospermia

We performed whole-exome sequencing on 30 men with infertility, 20 of whom presented with an MMAF phenotype and 10 of whom presented with only asthenozoospermia. Sequencing of the blood and sperm samples of a 29-year-old Tibetan man who had been infertile for two years and presented with severe asthenozoospermia showed that he carried a homozygous frameshift insertion (ENST00000313838.12: c.644dup) in the *DRC3* (*LRRC48*) gene, which was predicted to cause premature translational arrest of the *DRC3* protein (p.Glu216GlyfsTer36). Sanger sequencing confirmed the variant. In addition, Sanger sequencing of the patient's parents revealed that they are carriers of the mutation. His parents are consanguineous; therefore, the variant is likely to have autosomal recessive inheritance (Fig. 1A).

Human *DRC3* encodes LRRC48, which contains five LRR (1–5) domains, one LRR carboxy-terminal domain (LRRCT), and two coiled-coil domains. *DRC3* translates into a 523-amino acid protein (~ 61 kDa) (Fig. 1B). The glutamic acid at position 216 of *DRC3* is highly conserved from zebrafish to human (Fig. 1C).

Basic information and semen analysis of the patient

The patient had no children despite two years of regular and unprotected intercourse. In 2019, he underwent a semen examination at the Department of Andrology/Sichuan Human Sperm Bank of West China Second University Hospital. The results revealed that the semen color, pH, and concentration were normal, but the proportion of forward motile sperm was only 9%, and the total motility rate was 23% (Table 1). According to WHO guidelines (fifth edition), the normal percentage of progressive motility is at least 32%, and the total motility rate is greater than

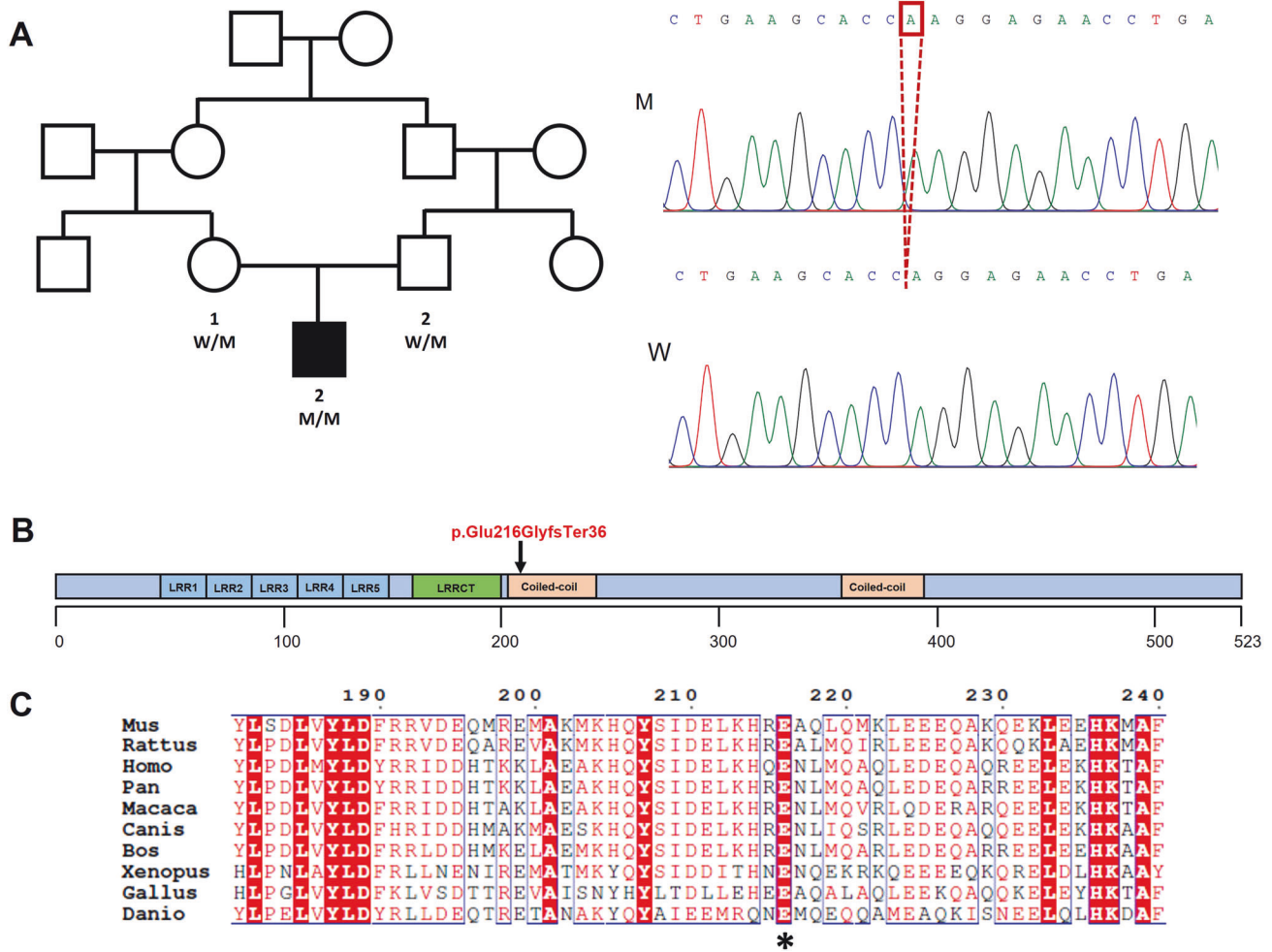


Fig. 1 Identification of homozygous *DRC3* mutation in a patient with asthenozoospermia. **A** Pedigree of the family and Sanger sequencing results. Circles indicate women, blank and black filled squares present normal men and the patient with asthenozoospermia. Sanger sequencing confirmed *DRC3* homozygous frame shift insertion mutation in the patient. **B** Structure diagram of *DRC3* protein and the location of the detected variant in *DRC3*. The numbers indicated the amino acids, the position of the mutation is indicated in the protein structure of *DRC3*, different domains of *DRC3* are marked, LRR1-5 represent the Leucine-rich repeats domains, LRRCT marked with green represents Leucine-rich repeats carboxy-terminal domain, pinkish-oranges indicate Coiled coil domains. **C** Conservation analysis of *DRC3* amino acid sequence in different species, asterisk shows the mutation site

Table 1. Semen parameters and in the patient

Semen parameters	Subject	Reference limits ^a
Color	Gray-white	Milk-white, gray-white
Semen volume (mL)	1.4	≥ 1.5
pH	7.5	7.2–8.5
Sperm count (M)	57.54	≥ 39
Sperm concentration (10 ⁶ /mL)	41.1	≥ 15
Total Motility (%)	23	≥ 40
Progressive motility (%)	9	≥ 32
Sperm morphology		
Normal (%)	5	≥ 4
Abnormal head (%)	94.5	/
Abnormal mid-piece (%)	0.3	/
Abnormal flagella (%)	0.2	/

The patient is 29 years old and has a normal karyotype

^aReference limits based on the fifth WHO standards; M, Million

40%. These findings indicate that the patient had severe asthenozoospermia. His karyotype was normal (46XY), as were his hormone levels, bilateral testicular size distribution, and secondary sex characteristics.

Morphology and abnormal ultrastructure of the patient's spermatozoa

The sperm structure consists four parts: head, midpiece, principal piece, and end piece. Among these, the sperm axoneme is evolutionarily highly conserved and is the structural basis of sperm motility. The midpiece includes a helical mitochondrial sheath, outer dense fibers, and an axoneme. A central pair of microtubules and nine DMTs make up the main structure of the axoneme, which is the typical "9 + 2" microtubule structure in normal cilia and flagella. Each pair of DMTs is composed of sub-microtubules A and B. Two rows of dynein motors are attached to the DMTs: the outer and inner dynein arms [4]. The N-DRC connects adjacent DMTs [17] (Fig. 2A).

The proportion of sperm with normal morphology was approximately 5%, just above the reference value of the WHO (normal morphology > 4%). Compared with normal controls, there

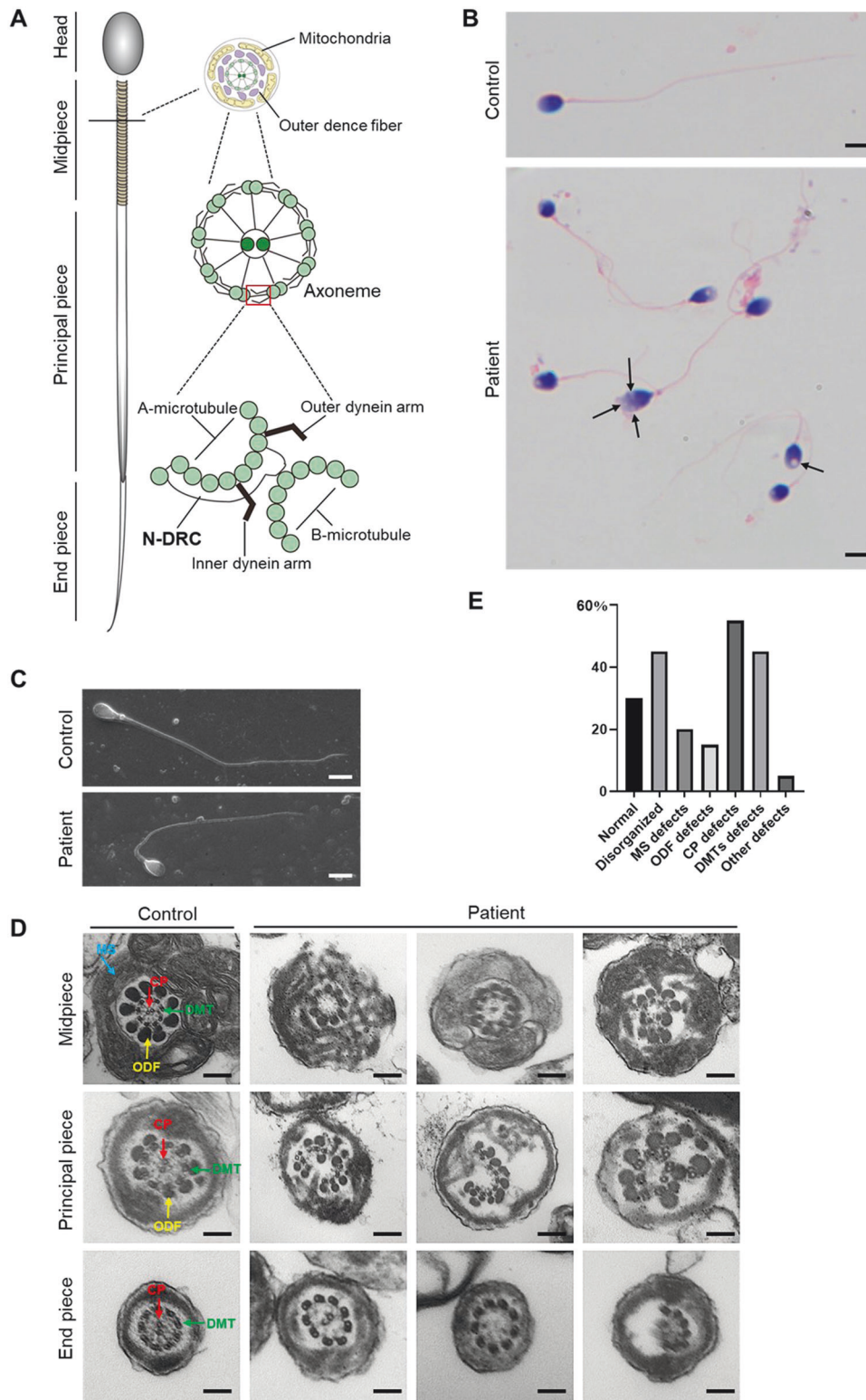


Fig. 2 Morphology and ultrastructure of the patient's sperm. **A** Schematic diagram of sperm structure and the modal of N-DRC complex location. **B** Papanicolaou staining results for a normal control and the patient. Black arrows: vacuoles. Scale bars: 5 μm. **C** SEM analysis of the sperm from the normal control and the patient. Scale bars: 5 μm. **D** TEM analysis of the sperm from the normal control and the patient. Cross-sections of the midpiece (upper), principal piece (middle) and end piece (lower) from the sperm flagella. CP: central pair of microtubules, red arrows; DMTs: doublet microtubules, green arrows; ODFs: outer dense fibers, yellow arrows; MS: mitochondrial sheath, blue arrows. Scale bars: 200 nm. **E** Statistical charts of different cross-section structures of the flagellar axoneme. Total cross-sections numbers for quantification in the normal control and the patient were 101 and 105 respectively

Table 2. Categories of defective spermatozoa with head, midpiece and principal piece abnormalities in the patient

Sperm defect categories	Percentage ^a (%)
Normal spermatozoa	5
Abnormal spermatozoa	95
Sperm defect categories^b	
Head defects	94.5
vacuolated	73
pyriform	6.7
Round or small acrosome	17.3
Midpiece defects	0.3
Thick insertion	0.2
thin	0.1
Tail defects	0.2
short	0.08
coiled	0.12

^aPercentage: defective sperm count/ total sperm count

^bSpecification of some sperm defect categories:

Vacuolated: sperm heads with more than two vacuoles, or one vacuole area occupies more than 20% of the head

Pyriform: sperm head is pear shaped

Thick insertion: sperm midpiece is thick

Thin: sperm midpiece is thin

Head defects include: vacuolated, pyriform, round or small acrosome

Midpiece defects include: thick insertion, thin

Tail defects include: short, coiled

were no apparent defects in the morphology of the tail of the patient's sperm. However, the head morphology was strictly abnormal (Fig. 2B), and the proportion of abnormal heads was approximately 94.5% (Table 1). Most sperm heads (approximately 73%) were defective in the acrosome and contained one large or multiple small vacuoles. Besides vacuoles, 17.3% sperm heads were with round or small acrosomes, and 6.7% were pyriform (Table 2). There are few reports on vacuoles in the sperm acrosome, and the exact mechanisms of vacuoles formation and function remain unclear. Therefore, it is worthy to explore the mechanisms and function of sperm vacuoles. SEM revealed that the surface of the sperm tail with the *DRC3* mutation was normal (Fig. 2C). However, on further investigation of the flagellar ultrastructure using TEM, the patient displayed severe defects, especially in the "9 + 2" structure (Fig. 2D). Even though 30% sperm had normal flagellar structure, 68% of flagellar axonemes displayed structure defects, including in the mitochondrial sheath (20%), outer dense fibers (15%), central pair of microtubules (55%), DMTs (45%), and others (5%); some cross-sections of flagellar axonemes displayed more than two types of defects or displayed disorganized (Fig. 2E). In contrast, most of the cross-sections of the normal control displayed an intact axoneme and structure, except for 10% that displayed incomplete or disorganized structures. These results indicate that *DRC3* plays a critical role in the flagellar ultrastructure.

Evaluation and localization of *DRC3*

Western blot was used to evaluate *DRC3* in the patient and fertile male control subjects. The results showed that the *DRC3* protein was specifically identified in the control but not in the patient's sperm (Fig. 3A). Quantitative real-time PCR revealed that *DRC3* was expressed primarily in the human testis, followed by the ovary and

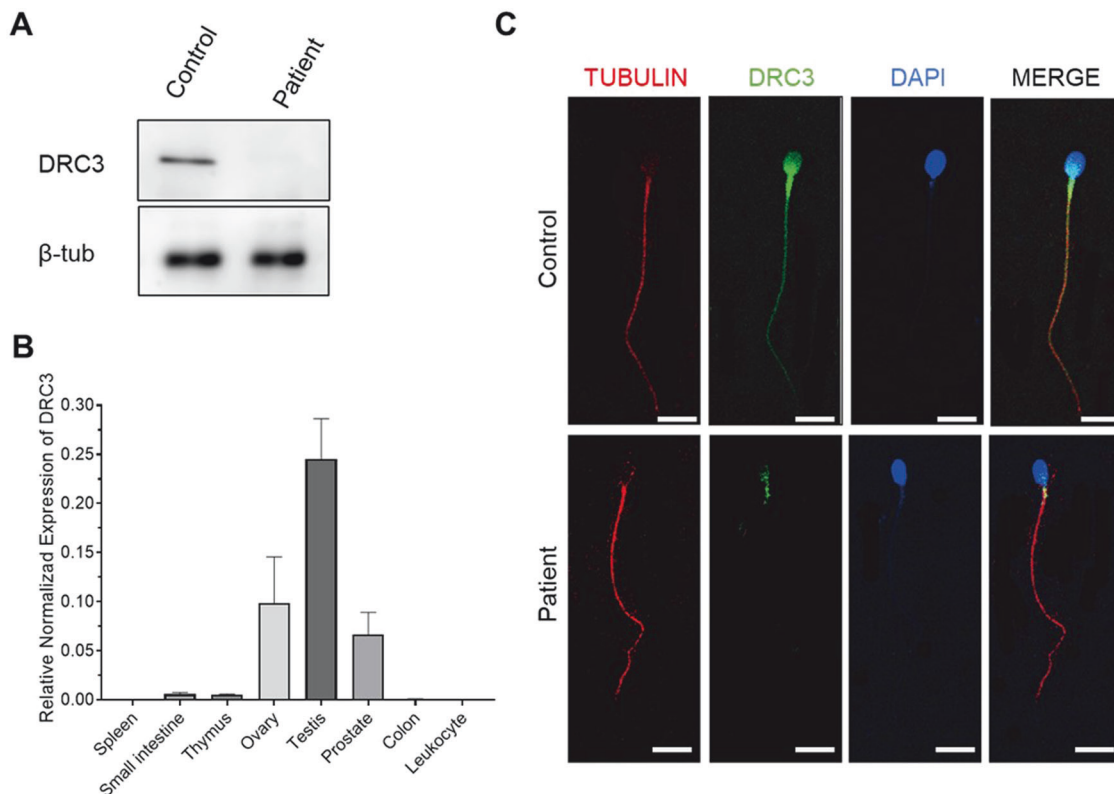
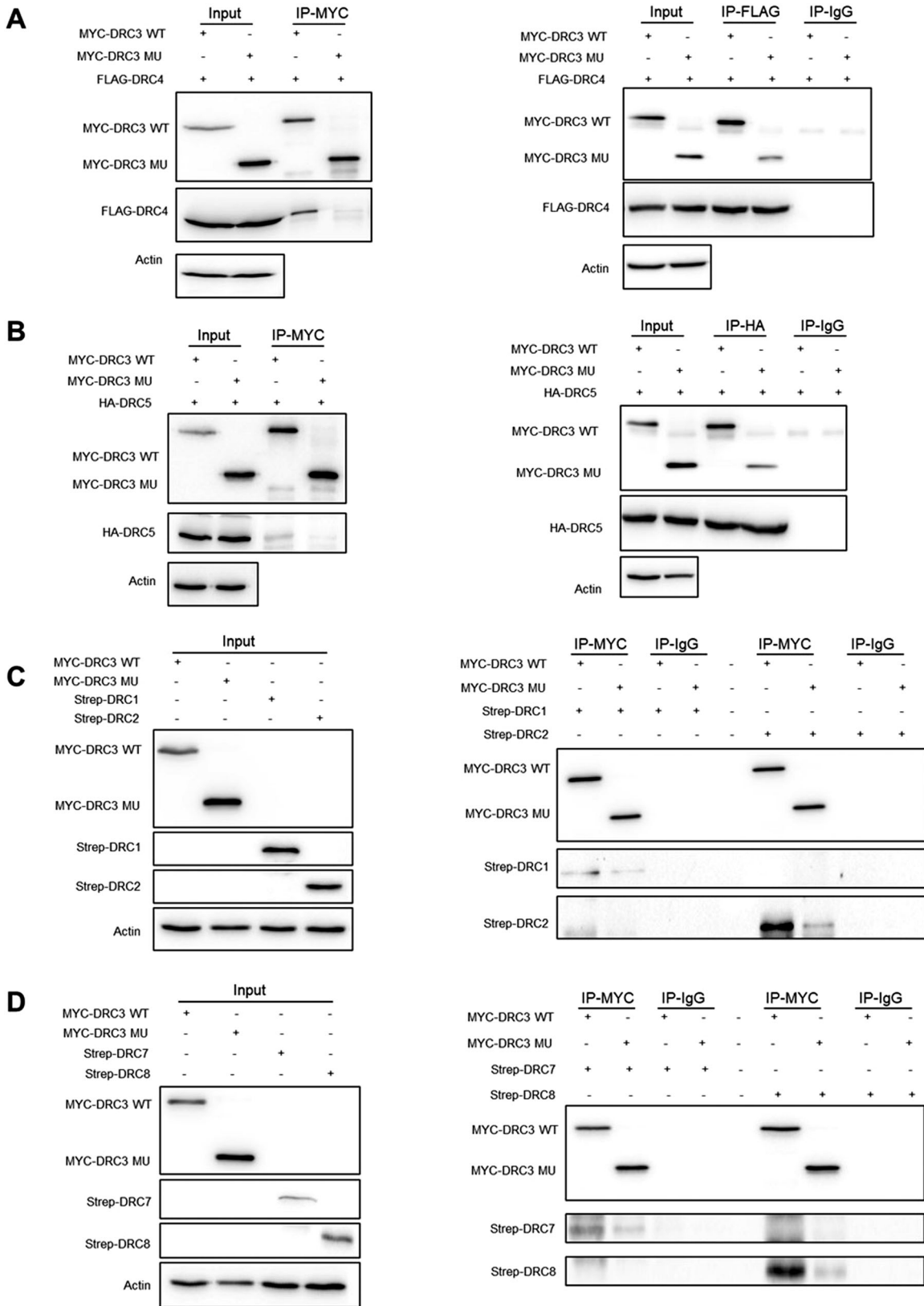


Fig. 3 Evaluation of *DRC3*. **A** Evaluation of *DRC3* in normal control and the patient by western blot. β -tub: β -tubulin. **B** Quantitative real-time PCR evaluated the expression of *DRC3* in human tissues. **C** Immunofluorescence analysis of *DRC3*. *DRC3* was labeled by FITC (green); Nuclei were labeled by DAPI (blue), and sperm flagella were marked by anti-tubulin (red). Scale bars: 5 μ m



prostate. It was rarely expressed in the spleen, small intestine, thymus, colon, or leukocytes (Fig. 3B). This suggests that *DRC3* may play an important role in spermatogenesis. Immunofluorescence analysis indicated that *DRC3* was normally localized along

the sperm flagella in the controls (there may be additional aspecific binding of the antibody to the sperm head). However, *DRC3* protein levels were markedly reduced in the patient's sperm (Fig. 3C).

Fig. 4 DRC3 variant reduced its interaction with DRC1, 2, 4, 5, 7, and 8. Transfected MYC-DRC3 WT/MU, FLAG-DRC4, HA-DRC5, Strep-DRC1, 2, 7, and 8 into HEK 293 F cells and incubated in 37 °C for 72 h. **A** MYC-DRC3 WT and MU co-immunoprecipitation with FLAG-DRC4. Cell lysate of MYC-DRC3 WT/MU were mixed with FLAG-DRC4, anti-MYC (left) or anti-FLAG (right) beads were used. The control was mixed with anti-IgG beads. **B** MYC-DRC3 WT and MU co-immunoprecipitation with HA-DRC5. MYC-DRC3 WT/MU HEK 293 F cell lysate were mixed with anti-MYC (left) or anti-HA (right) beads and co-immunoprecipitation with FLAG-DRC5. The control was mixed with anti-IgG beads. **C** MYC-DRC3 WT/MU co-immunoprecipitation with Strep-DRC1/DRC2. The experimental assay was the same as **A**. **D** Co-immunoprecipitation of MYC-DRC3 WT/MU with Strep-DRC7/DRC8. The experimental assay was the same as **A**

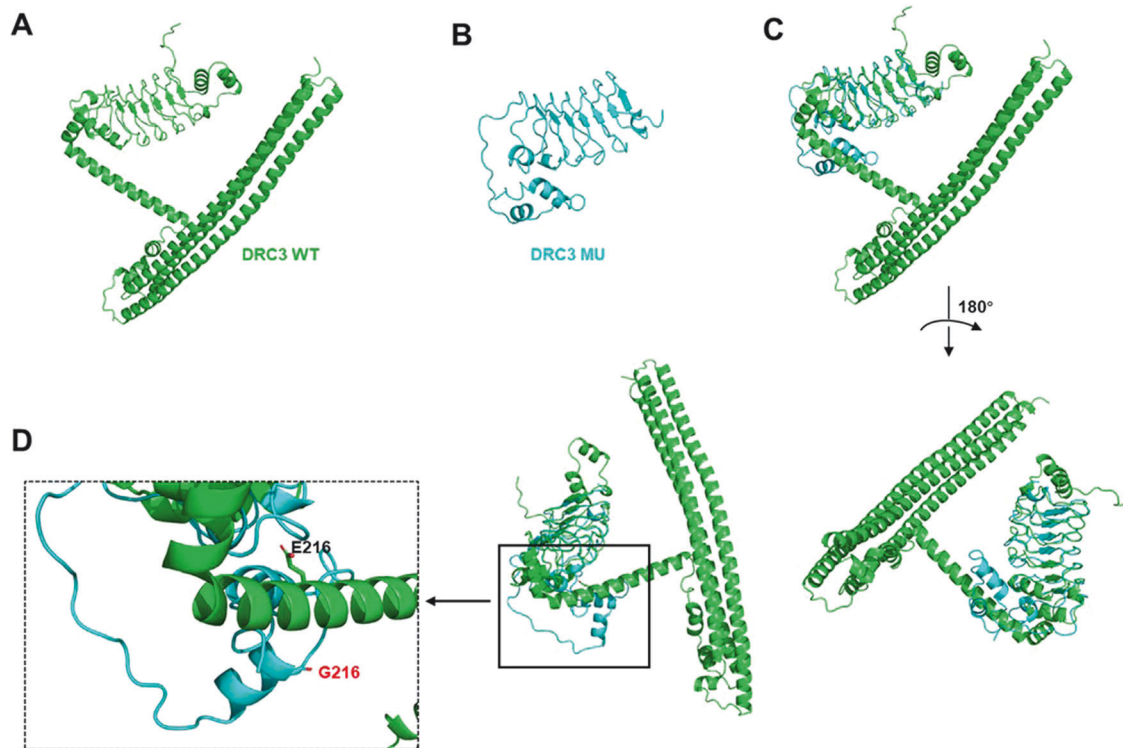


Fig. 5 The structure models of DRC3 WT and MU. The 3D structures of DRC3 WT **A** and MU **B** were predicted by Alpha-Fold. **C** The DRC3 WT and MU structures were aligned and showed in two orientations rotated 180° with respect of each other. Green represents DRC3 WT, blue represents DRC3 MU. **D** Amplification of variant site in DRC3 MU. E216 (black) indicates glutamic acid at position of 216 in DRC3 WT, G216 (red) indicates glycine at position of 216 in DRC3 MU

DRC3 mutation diminishes its interaction with other N-DRC components

Previous studies have shown that DRC3 interacts with DRC4 and DRC5 in vitro [3, 18]. We transfected MYC-DRC3, FLAG-DRC4 and HA-DRC5 into HEK 293 F cells and conducted co-immunoprecipitation experiments to confirm the interaction of DRC3 and the mutated form of DRC3 (DRC3 MU) with DRC4 or DRC5 in vitro. When MYC-DRC3 WT or DRC3 MU was used to pull down DRC4/DRC5, the interaction of the DRC3 MU with DRC4 or DRC5 was significantly weakened compared with the wild type, the results were the same when DRC4/DRC5 was used to pull down MYC-DRC3 WT or DRC3 MU (Fig. 4A, 4B). To further investigate the effects of DRC3 MU on other N-DRC components, we expressed Strep-DRC1, 2, and Strep-DRC6-11 in 293 F cells, but only Strep-DRC1, 2, 7, and 8 were expressed normally. We then used MYC-DRC3 WT or DRC3 MU to pull down Strep-DRC1, 2, 7, and 8. Compared with the wild type, the DRC3 MU had weaker interactions with DRC1, 2, 7 and 8 (Fig. 4C, 4D).

Using Alpha-Fold, we predicted the tertiary structure of DRC3 WT and DRC3 MU (Fig. 5A, 5B). By fitting the two structures, we found mutation loss of three-helix bundles in the C-terminus. However, the structure of the N-terminus of the DRC3 mutant did not change significantly (Fig. 5C, 5D). These results indicate that the mutation of DRC3 may change the tertiary structure of the DRC3 protein, affecting its interaction with other N-DRC components.

DISCUSSION

Here, using whole-exome sequencing to conduct genetic testing of 30 unrelated male patients with low sperm motility, we identified a novel homozygous variant of *DRC3* in a Tibetan patient, who was diagnosed with asthenozoospermia and male infertility at the Department of Andrology/Sichuan Human Sperm Bank, West China Second University Hospital, in China. The ENST00000313838.12: c.644dup variant caused premature translational arrest of DRC3, resulting in a loss-of-function DRC3 protein (p.Glu216GlyfsTer36).

Mutations in N-DRC subunits usually cause defects in flagellar motility resulting in primary ciliary dyskinesia, male infertility, and random determination of visceral asymmetry [3, 10, 18–25]. In the present study, the patient did not present with any symptoms of primary ciliary dyskinesia other than asthenozoospermia and infertility.

DRC3 is a component of the N-DRC, and *DRC3* mutations were first characterized in *Chlamydomonas* [9]. In 1982, through proteomics analysis of flagellar axonemal polypeptides, *DRC3-11* were found to be missing in *pf2*, and *DRC3-9* and *11* were reduced in *sup-pf-3* of *Chlamydomonas* [26]. These *DRC3* mutants affect the entire proximal and distal lobes of the N-DRC structure [27]. A *drc3* mutant in *Chlamydomonas* affects only the DRC3 subunit of N-DRC, which lacks a portion of the N-DRC linker domain, resulting in an abnormal flagellar waveform associated with reduced swimming speed [9]. This provides direct evidence for the importance of *DRC3* in flagellar

motility [5, 9, 28]. *LRR48* is an ortholog of *DRC3* in mammals. A recent study identified two bi-allelic *DRC3* frameshift variants in two unrelated patients. The two mutations in the two patients were inherited from their respective parents carrying the heterozygous mutations. Patient 1 displayed an MMAF phenotype and showed a dramatic decrease in total and progressive motility. Due to an inguinal herniorrhaphy in childhood, patient 2 displayed obstructive azoospermia. Using phase contrast microscopy, spermatozoa from percutaneous epididymal sperm aspiration of patient 2 showed an MMAF phenotype. *DRC3* knockout mouse models also displayed male infertility and MMAF. These results demonstrated that defects in *DRC3* were closely related with MMAF [10]. However, our present study identified a *DRC3* mutation in one patient who did not show the MMAF phenotype but displayed asthenozoospermia, which differed from the reported phenotype in the two patients and *DRC3* knockout mice. These findings provide an improved basis for diagnosing of male infertility with asthenozoospermia. Although the sperm flagella of the patient in our study did not display obvious defects, the ultrastructure was considerably destroyed. It is possible that the surface structure of the sperm flagella can be intact despite the ultrastructure being disrupted, which destroys sperm motility. One of the two reported *DRC3* mutations resulted in a 41-base pair deletion at the junction of exon 6, and the other resulted in a deletion in exons 11–14 of *DRC3*, both of which caused frameshift variants [10]. The mutation in our study hit exon 7 and also caused a frameshift variant, mutations in the reported patient 1 and our study, as well as *DRC3* knockout mice resulted in *DRC3* protein lost. *DRC3* is the adapter required for functional subunits of the N-DRC, therefore, we speculated that changes in the tertiary structure of *DRC3* affect its stability. However, the specific mechanism needs to be further studied. In the reported study, the *DRC3*-gene knockout mice and one patient produced healthy offspring via intracytoplasmic sperm injection treatment, which demonstrated that this recessively inherited disease can be overcome [10]. Further studies are needed to collect additional sperm samples with normal flagellar morphotypes and reduced motility. Furthermore, the fertility outcomes of these patients should be tracked.

The atomic models of N-DRC have become increasingly detailed with the development of cryo-electron microscopy. Recently, Walton et al. described the atomic models of the 11 subunits of N-DRC. All the subunits are built around long coiled coils that are bifurcated and joined together at a “bulb” on the microtubule-bound baseplate and fork at the N-terminal leucine-rich repeat domain of *DRC3*. Coiled coils of *DRC1*-*DRC2* and *DRC4*-*DRC4* curve proximally and provide binding sites for *DRC5*, 7, and 11. *DRC6* and *DRC9*-*DRC10* are located on the distal tip and point an additional 26 lysine residues toward neighboring DMTs. *DRC8* binds to *DRC9* and *DRC11* [29]. In our study, the tertiary structure of the *DRC3* mutation was destroyed, and the mutation showed weaker interaction with other N-DRC subunits (*DRC1*, 2, 4, 5, 7, and 8). In addition, our results showed that *DRC3* can interact with *DRC8*, and the interaction between *DRC3* MU and *DRC8* is weaker than that with *DRC3* WT, which contradicts existing results. Next, we will focus on the exact structures of *DRC3* and *DRC8* to verify the reported structure of the N-DRC. Overall, *DRC3* plays a key role in flagellar functions.

In this study, we identified a homozygous variant of the *DRC3* gene in an infertile man with asthenozoospermia. The mutation did not change the morphology of the sperm flagella but destroyed its ultrastructure. In addition, the *DRC3* variant reduced its interaction with other N-DRC subunits. These findings revealed a mechanism of *DRC3* deficiency in the asthenozoospermia phenotype, which could provide a new basis for diagnosing male infertility.

REFERENCES

- Bhasin S, de Kretser DM, Baker HW. Clinical review 64: pathophysiology and natural history of male infertility. *J Clin Endocrinol Metab.* 1994;79:1525–9.
- Ford WC. Comments on the release of the 5th edition of the WHO Laboratory Manual for the Examination and Processing of Human Semen. *Asian J Androl.* 2010;12:59–63.
- Castaneda JM, Hua R, Miyata H, Oji A, Guo Y, Cheng Y, et al. TCTE1 is a conserved component of the dynein regulatory complex and is required for motility and metabolism in mouse spermatozoa. *Proc Natl Acad Sci USA.* 2017;114:E5370–E78.
- Inaba K. Molecular basis of sperm flagellar axonemes: structural and evolutionary aspects. *Ann N. Y Acad Sci.* 2007;1101:506–26.
- Heuser T, Raytchev M, Krell J, Porter ME, Nicastro D. The dynein regulatory complex is the nexin link and a major regulatory node in cilia and flagella. *J Cell Biol.* 2009;187:921–33.
- Bower R, Tritschler D, Vanderwaal K, Perrone CA, Mueller J, Fox L, et al. The N-DRC forms a conserved biochemical complex that maintains outer doublet alignment and limits microtubule sliding in motile axonemes. *Mol Biol Cell.* 2013;24:1134–52.
- Ghaneaian A, Majhi S, McCafferty CL, Nami B, Black CS, Yang SK, et al. Integrated modeling of the Nexin-dynein regulatory complex reveals its regulatory mechanism. *Nat Commun.* 2023;14:5741.
- Lin J, Tritschler D, Song K, Barber CF, Cobb JS, Porter ME, et al. Building blocks of the nexin-dynein regulatory complex in Chlamydomonas flagella. *J Biol Chem.* 2011;286:29175–91.
- Awata J, Song K, Lin J, King SM, Sanderson MJ, Nicastro D, et al. *DRC3* connects the N-DRC to dynein g to regulate flagellar waveform. *Mol Biol Cell.* 2015;26:2788–800.
- Zhou S, Yuan S, Zhang J, Meng L, Zhang X, Liu S, et al. *DRC3* is an assembly adapter of the nexin-dynein regulatory complex functional components during spermatogenesis in humans and mice. *Signal Transduct Target Ther.* 2023;8:26.
- Chen J, Zhang P, Chen H, Wang X, He X, Zhong J, et al. Whole-genome sequencing identifies rare missense variants of *WNT16* and *ERVW-1* causing the systemic lupus erythematosus. *Genomics.* 2022;114:110332.
- Oud MS, Houston BJ, Volozonoka L, Mastroianni FK, Holt GS, Alobaidi BKS, et al. Exome sequencing reveals variants in known and novel candidate genes for severe sperm motility disorders. *Hum Reprod.* 2021;36:2597–611.
- Jia Y, Chen J, Zhong J, He X, Zeng L, Wang Y, et al. Novel rare mutation in a conserved site of PTPRB causes human hypoplastic left heart syndrome. *Clin Genet.* 2023;103:79–86.
- Hubbard T, Barker D, Birney E, Cameron G, Chen Y, Clark L, et al. The Ensembl genome database project. *Nucleic Acids Res.* 2002;30:38–41.
- Pereira R, Carvalho V, Dias C, Barbosa T, Oliveira J, Alves A, et al. Characterization of a *DRC1* null variant associated with primary ciliary dyskinesia and female infertility. *J Assist Reprod Genet.* 2023;40:765–78.
- Zhang X, Wang L, Ma Y, Wang Y, Liu H, Liu M, et al. *CEP128* is involved in spermatogenesis in humans and mice. *Nat Commun.* 2022;13:1395.
- Oda T, Yanagisawa H, Kikkawa M. Detailed structural and biochemical characterization of the nexin-dynein regulatory complex. *Mol Biol Cell.* 2015;26:294–304.
- Jeanson L, Thomas L, Copin B, Coste A, Sermet-Gaudelus I, Dastot-Le Moal F, et al. Mutations in *GAS8*, a gene encoding a nexin-dynein regulatory complex subunit, cause primary ciliary dyskinesia with axonemal disorganization. *Hum Mutat.* 2016;37:776–85.
- Lei C, Yang D, Wang R, Ding S, Wang L, Guo T, et al. *DRC1* deficiency caused primary ciliary dyskinesia and MMAF in a Chinese patient. *J Hum Genet.* 2022;67:197–201.
- Keicho N, Hijikata M, Morimoto K, Homma S, Taguchi Y, Azuma A, et al. Primary ciliary dyskinesia caused by a large homozygous deletion including exons 1–4 of *DRC1* in Japanese patients with recurrent sinopulmonary infection. *Mol Genet Genom Med.* 2020;8:e1033.
- Olbrich H, Cremers C, Loges NT, Werner C, Nielsen KG, Marthin JK, et al. Loss-of-function *GAS8* mutations cause primary ciliary dyskinesia and disrupt the nexin-dynein regulatory complex. *Am J Hum Genet.* 2015;97:546–54.
- Morohoshi A, Miyata H, Shimada K, Nozawa K, Matsumura T, Yanase R, et al. Nexin-Dynein regulatory complex component *DRC7* but not *FBXL13* is required for sperm flagellum formation and male fertility in mice. *PLoS Genet.* 2020;16:e1008585.
- Zhang J, He X, Wu H, Zhang X, Yang S, Liu C, et al. Loss of *DRC1* function leads to multiple morphological abnormalities of the sperm flagella and male infertility in human and mouse. *Hum Mol Genet.* 2021;30:1996–2011.
- Takeuchi K, Xu Y, Kitano M, Chiyonobu K, Abo M, Ikegami K, et al. Copy number variation in *DRC1* is the major cause of primary ciliary dyskinesia in the Japanese population. *Mol Genet Genom Med.* 2020;8:e1137.
- Zhou S, Wu H, Zhang J, He X, Liu S, Zhou P, et al. Bi-allelic variants in human *TCTE1/DRC5* cause asthenospermia and male infertility. *Eur J Hum Genet.* 2022;30:721–29.
- Huang B, Ramanis Z, Luck DJ. Suppressor mutations in *Chlamydomonas* reveal a regulatory mechanism for flagellar function. *Cell.* 1982;28:115–24.

27. Luck DJ, Huang B, Piperno G. Genetic and biochemical analysis of the eukaryotic flagellum. *Symp Soc Exp Biol.* 1982;35:399–419.
28. Piperno G, Mead K, LeDizet M, Moscatelli A. Mutations in the “dynein regulatory complex” alter the ATP-insensitive binding sites for inner arm dyneins in *Chlamydomonas axonemes*. *J Cell Biol.* 1994;125:1109–17.
29. Walton T, Gui M, Velkova S, Fassad MR, Hirst RA, Haarman E, et al. Axonemal structures reveal mechanoregulatory and disease mechanisms. *Nature.* 2023;618:625–33.

ACKNOWLEDGEMENTS

We wish to thank the patient and medical staff of Department of Andrology/Sichuan Human Sperm Bank, West China Second University Hospital.

AUTHOR CONTRIBUTIONS

Jiao Qin designed the study and wrote the paper. Jinyu Wang performed the experiments and analyzed the data. Jianhai Chen analyzed the sequencing data and identified the variant gene. Jinyan Xu collected clinical samples and signed informed consent with human subjects, Fuping Li, Dong Deng and Shanling Liu directed this study.

FUNDING

This study was supported by the Clinical Discipline Development Fund, West China Second University Hospital of China (KL061).

COMPETING INTERESTS

The authors declare that the research was conducted without any commercial or financial relationships that could be construed as a potential conflict of interest.

ETHICS

The study was reviewed and approved by Review Board of the West China Second University Hospital in China, Number 2020-102. All human subjects provided informed consent for this study.

ADDITIONAL INFORMATION

Correspondence and requests for materials should be addressed to Shanling Liu, Dong Deng or Fuping Li.

Reprints and permission information is available at <http://www.nature.com/reprints>

Publisher's note Springer Nature remains neutral with regard to jurisdictional claims in published maps and institutional affiliations.

Springer Nature or its licensor (e.g. a society or other partner) holds exclusive rights to this article under a publishing agreement with the author(s) or other rightsholder(s); author self-archiving of the accepted manuscript version of this article is solely governed by the terms of such publishing agreement and applicable law.